

Epoxidation of Styrene with H₂O₂ Catalyzed by Alanine–Salicylaldehyde Schiff Base Chromium (III) Complexes Immobilized on Mesoporous Materials

Xiaoli Wang · Gongde Wu · Wei Wei ·
Yuhan Sun

Received: 9 August 2009 / Accepted: 5 February 2010 / Published online: 24 February 2010
© Springer Science+Business Media, LLC 2010

Abstract Alanine–salicylaldehyde Schiff base chromium (III) complex was immobilized on mesoporous silica gel (SiO₂), MCM-41 and SBA-15. The resulting immobilized complexes were promising catalysts for the epoxidation of styrene with 30% hydrogen peroxide, and they all showed much higher catalytic performance than their homogeneous analogue. Simultaneously, the catalytic performance of immobilized complexes was found to be closely related to the textual and surface properties of the supports used. The complex immobilized on methyl-containing MCM-41 exhibited the highest catalytic performance. Under optimal reaction conditions, the highest conversion of styrene reached 80.2% with 77.0% selectivity to epoxide. In addition, the catalytic performance remained stable after six times of recycling.

Keywords Chromium complexes · Immobilized · Mesoporous materials · Styrene · Epoxidation

Electronic supplementary material The online version of this article (doi:10.1007/s10562-010-0301-8) contains supplementary material, which is available to authorized users.

X. Wang · G. Wu (✉)
Department of Environment and Technology, Nanjing Institute of Technology, 211167 Nanjing, People's Republic of China
e-mail: wugongde@njit.edu.cn

X. Wang
e-mail: wangxiaoli212@126.com

W. Wei · Y. Sun
State Key Laboratory of Coal Conversion, Institute of Coal Chemistry, Chinese Academy of Sciences, 030001 Taiyuan, People's Republic of China

1 Introduction

Catalytic epoxidation of alkenes to epoxides is a versatile reaction from a synthetic point of view. Epoxides can be easily converted into polyethers, diols and aminoalcohols, which are of great importance in bulk chemistry, fine chemistry and pharmaceutical industry [1]. Though a large number of methods have been developed for the conversion of alkenes to epoxide, only a few useful catalytic systems with H₂O₂ as oxidant have been reported [2–8]. Therefore, there is an urgent need to develop effective catalysts for the epoxidation with H₂O₂.

Transition metal Schiff base complexes bear resemblance to enzymatic catalysts and are eye-catching since they provide advantages due to their relatively easy synthesis and versatile coordination structures. Among the various transition metal complexes reported [9–17], the amino acid Schiff base complexes have been proven to be excellent catalysts for catalytic epoxidation [13, 14]. However, such homogeneous complexes suffer from the drawbacks of poor catalyst recovery and product separation [18]. Thus, in the past decade, much effort has been paid to immobilize the homogeneous catalysts onto various supports, especially the siliceous mesoporous materials [19–21]. The method used frequently was to immobilize the active homogeneous complexes on supports through surface-bound linkers [22]. In order to tailor the immobilized catalysts for the desired performance, several groups investigated the role of linkers, supports and immobilization methods to improve the catalytic performance. Lau et al. reported that the dispersion effect of supports played an important role in the catalytic performance of immobilized complexes [23]. Corma and coworkers demonstrated that the linker length and immobilized methods influenced the catalytic performance of immobilized

complexes [24, 25]. We have also reported on the importance of the linker flexibility and the coordination abilities of terminal functional groups in linkers [26]. However, to the best of our knowledge, there are few reports which systemically deal with the effect of the textural and surface properties of supports such as their channels, pore sizes, surface area, surface polarity and hydrophobicity on the catalytic performance of immobilized complexes.

Here we report the epoxidation of styrene with 30% H₂O₂ catalyzed by a series of alanine–salicylaldehyde Schiff base chromium (III) complexes immobilized on three typical mesoporous supports. Moreover, the roles of the textural and surface properties of supports in the catalytic performance of immobilized complexes are discussed in detail.

2 Experimental

2.1 Catalyst Preparation

2.1.1 Preparation of Aminopropyl Functionalized Supports (APTES-Supports)

SiO₂ was purchased from Shanghai Chemical Reagent Company. The pure siliceous MCM-41 and SBA-15 were synthesized as previously described [27, 28]. Aminopropyl functionalized supports (APTES–SiO₂, APTES–MCM-41 and APTES–SBA-15) were prepared as in the literature [25].

2.1.2 Preparation of Methyl-Containing APTES-Supports (APTES-Support(CH₃))

The methyl-containing APTES-supports were prepared by following the procedures in our previous report [29]. Typically, the as-prepared APTES-support (3 g) was degassed at 50 °C under 10⁻² Pa for 2 h. Then, an excess of dimethyldiethoxysilane (0.03 mol) in dry toluene (100 mL) was added, and the suspension was stirred at reflux temperature under nitrogen flow for 24 h. The resulting solid was filtered, Soxhlet-extracted with dichloromethane for 24 h and dried in air (at 60 °C under 10⁻² Pa for 3 h). Then, the corresponding methyl-containing supports were obtained and denoted as APTES–SiO₂(CH₃), APTES–MCM-41(CH₃) and APTES–SBA-15(CH₃).

2.1.3 Preparation of the Homogeneous Alanine–Salicylaldehyde Schiff base Chromium (III) Complex (Cr(Sal–Ala))

The synthetic procedures for the homogeneous Cr(Sal–Ala) complex were similar as those reported in references

[30, 31]. The ligand Sal–Ala was prepared firstly by condensation of salicylaldehyde and β-alanine with a salicylaldehyde/alanine at molar ratio of 1. Typically, alanine (0.02 mol) was suspended in 60 mL of deionized water. Then salicylaldehyde (0.02 mol) dissolved in 60 mL absolute ethanol was added dropwise while vigorous stirring the suspension. After refluxing for 3 h, the resulting mixture was cooled, and produced precipitates upon addition of ether. To obtain crystals of the desired Schiff base ligand, the solid was further recrystallized from ethanol. Then, the ligand Sal–Ala (1.93 g) was dissolved in 50 mL absolute ethanol. The resultant solution was alkalized with the appropriate amount of NaOH to adjust the pH close to 7. A solution of CrCl₃·6H₂O (2.66 g) in 50 mL ethanol was added dropwise while stirring vigorously the above mixture so that the bright yellow solution turned green. After refluxing for 6 h, the solid was filtered, washed with cold ethanol, dried under vacuum (at 60 °C and 10⁻² Pa for 2 h) and recrystallized in absolute ethanol.

2.1.4 Preparation of the Heterogenised Chromium (III) Complexes

Typically, the solution of the as-prepared homogeneous complex (1.5 g) in 50 mL of dry toluene was added to the suspension of freshly dried APTES-support or APTES-support(CH₃) (1 g) in 50 mL of dry toluene. The mixture was vigorously stirred under reflux for 10 h. Then the resulting suspension was cooled and filtered through a Buchner funnel supplied with a fine-porous filter paper. The collected powder was washed overnight in a Soxhlet extractor using equivalent alcohol and acetonitrile as solvent to remove the homogeneous complexes adsorbed on the surface of the support, and then the solid was dried in air at 80 °C for 10 h. By choosing the different supports: APTES–SiO₂, APTES–MCM-41, APTES–SBA-15, APTES–SiO₂(CH₃), APTES–MCM-41(CH₃) and APTES–SBA-15(CH₃), the corresponding immobilized materials were obtained and denoted as Cr(Sal–Ala)–SiO₂, Cr(Sal–Ala)–MCM-41, Cr(Sal–Ala)–SBA-15, Cr(Sal–Ala)–SiO₂(CH₃), Cr(Sal–Ala)–MCM-41(CH₃) and Cr(Sal–Ala)–SBA-15(CH₃), respectively.

2.2 Characterization

The contents of carbon and nitrogen in the samples were determined using a Vario EL analyzer. The chromium contents were measured by inductively coupled plasma (ICP) emission spectroscopy (PerkinElmer ICP OPTIMA-3000). Powder X-ray diffraction (XRD) experiments were performed at room temperature on a Rigaku D Max III VC instrument with Ni filtered Cu K α radiation ($\lambda = 1.5404 \text{ \AA}$) at 40 kV and 30 mA, in the 2θ range of

1–9° at a scan rate of 1°/min. The specific surface area and average pore diameter were measured by N₂ adsorption–desorption using a Micromeritics ASAP-2000 instrument (Norcross, GA). The samples were outgassed at 80 °C and 10^{−4} Pa overnight and then the adsorption–desorption isotherms were measured at liquid nitrogen temperature. The surface area was calculated by the BET method and the average pore diameter was calculated by the BJH method from the desorption isotherm. Water adsorption isotherms were measured gravimetrically using a BELSORP 18 instrument (Bel Japan Inc.) at room temperature. Before the adsorption experiments, samples were pretreated at 110 °C for 6 h under vacuum. FTIR spectra of samples were recorded in KBr disks at room temperature on a Shimadzu (model 8201 PC) spectrophotometer. UV–Vis absorption spectra were recorded on a Shimadzu (model 2501 PC) spectrophotometer (for solid sample, optical grade BaSO₄ was used as reference). Solid state NMR spectra were recorded on a Bruker MSL 300 NMR spectrometer with resonance frequencies of 75.5 and 59.6 MHz for ¹³C and ²⁹Si, respectively. Chemical shifts (ppm) are reported relative to the external standard of tetramethylsilane. The hydrophobicity of methyl-containing immobilized complexes was typically tested by measuring the contact angle (θ) of a water droplet placed on the sample surface, using the formula: $\theta = \tan^{-1}(2h/W)$, where h is the height of the water droplet and W is the width of the droplet touching the samples surface [32].

2.3 Catalytic Test

The oxidation of styrene was carried out in a 100 mL Teflon-lined and magnetically stirred autoclave. In a typical experiment, a mixture of 0.25 g heterogenised catalyst or 0.025 g homogeneous complex and 0.025 mol styrene was stirred for about 10 min, and then the corresponding amount of 30% H₂O₂ was introduced. The autoclave was adjusted to the desired temperature within 5 min. After the reaction run for 2–16 h, the products were filtered out from the catalyst and then analyzed using a gas chromatograph with a capillary 30 m HP-5 column and an FID detector.

2.4 Adsorption Test

Typically, 0.05 g immobilized material was mixed separately with the solution A (8.0 × 10^{−8} mol styrene in 15 mL *n*-hexane) and B (8.0 × 10^{−8} mol epoxide in 15 mL *n*-hexane). After stirring at 0 °C for 4 h, the mixtures were filtered and the UV–Vis absorptions of the filtrate solutions were recorded. The concentrations were determined on the basis of UV–Vis spectra and compared with standard solutions.

3 Results and Discussion

3.1 NMR Spectra of Organo-Modified Supports

Typical NMR spectra of APTES–MCM-41 and APTES–MCM-41(CH₃) are shown in Figs. 1, 2. In the ²⁹Si NMR spectrum of APTES–MCM-41 (see Fig. 1), the two resonances at about −109 and −99 ppm can be attributed to ²⁹Si nuclei having four Si–O–Si linkages (Q₄) and ²⁹Si nuclei having three Si–O–Si linkages and one –OH (Q₃), respectively. The two resonances at about −55 and −65 ppm are assigned to RSi(OSi)(OH)₂ and RSi(OSi)₃, respectively [33]. The presence of those characteristic resonances indicates the successful preparation of APTES–MCM-41. For APTES–MCM-41(CH₃), the characteristic resonances originating from APTES–MCM-41 are all present and simultaneously, two new resonances at about −6.5 and −13 ppm, corresponding to the attached Si(Me)₂ moiety [34], are also observed. This suggests that the methyl groups have been successfully introduced.

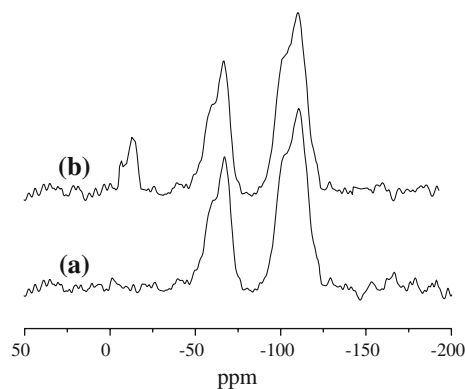


Fig. 1 ²⁹Si CP MAS NMR spectra of (a) APTES–MCM-41, (b) APTES–MCM-41(CH₃)

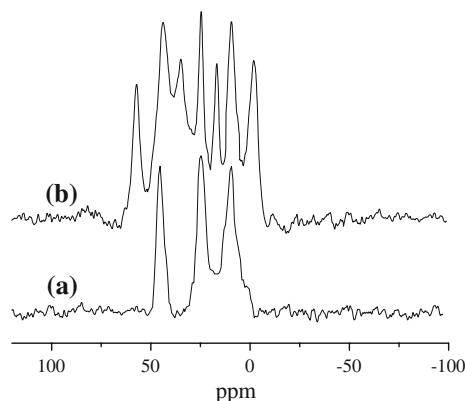


Fig. 2 ¹³C CP MAS NMR spectra of (a) APTES–MCM-41, (b) APTES–MCM-41(CH₃)

In the ¹³C NMR spectrum of APTES–MCM-41 (see Fig. 2), three peaks with almost equal intensity are observed at about 9.5, 22 and 43 ppm, respectively, which can be attributed to the three different C-atoms of the aminopropyl group [33]. This also indicates the successful anchoring of aminopropyl groups on the surface of the support. In the spectrum of APTES–MCM-41(CH₃), besides the characteristic resonances of APTES–MCM-41, four new resonances at about –1.7, 16.8, 35 and 57.3 ppm originating from methylated species are also found [35], further confirming the successful introduction of methyl groups.

3.2 Coordination Structures of Immobilized Materials

The results of the elemental analysis reveal that the obtained values of Cr(Sal–Ala) complex are quite comparable with the calculated ones (see Table 1), indicating that the as-prepared homogeneous complex maintains the expected elemental composition. The N/Cr molar ratios of all immobilized complexes are well consistent with the expected value of 2, which provides a supporting evidence for the successful immobilization of the homogeneous complex on the supports. Furthermore, a much higher carbon content in Cr(Sal–Ala)-support(CH₃) than in Cr(Sal–Ala)-support is also indicative of the successful introduction of methyl groups.

The FTIR spectrum of the homogeneous Cr(Sal–Ala) complex shows the characteristic bands at 1621 ($\nu_{\text{C=N}}$), 1570 ($\nu_{\text{as(COO}^-)}$), 1400 ($\nu_{\text{s(COO}^-)}$), 1332 ($\nu_{\text{(ph-O)}}$), 661 ($\nu_{\text{(Cr-O)}}$ (phenolic)), 612 ($\nu_{\text{(Cr-O)}}$ (carboxylic)) and 463 cm^{–1} ($\nu_{\text{(Cr-N)}}$) (see Fig. 3). This agrees well with the published literature data [31, 36], indicating the successful

preparation of the homogeneous complex. In the FTIR spectra of the immobilized complexes, apart from the bands in the overlapping regions of the silica backbone, the other bands of Cr(Sal–Ala) complex are all clearly observed despite some marginal shifts in the position of bands due to the immobilization. Thus the coordination structure of the homogeneous complex has survived the immobilization.

The UV–Vis spectrum of the homogeneous complex displays a peak at about 382 nm typical of the metal–ligand band and a broad peak at about 600 nm associated with a d–d transition (see Fig. 4). This is similar to related metal (Sal–Ala) compounds described in the literatures [37], also implying the successful preparation of the Cr(Sal–Ala) complex. The UV–Vis spectra of all immobilized materials are quite similar to the spectrum of the homogeneous complex, further confirming that the immobilized complexes as depicted in Scheme 1 were all successfully prepared.

3.3 Textural Properties of Immobilized Complexes

The powder XRD patterns of the complexes immobilized on MCM-41 and on SBA-15 show one single peak around 2 θ angles of 2–3° and 1–2°, respectively (see Fig. 5). This peak can be attributed to the (100) plane of the hexagonal unit cell, indicating that the structural ordering of parent MCM-41 and SBA-15 channels remains intact after the immobilization of the Cr(Sal–Ala) complex. However, the higher angle peaks associated with (110) and (200) reflections present in their parent samples no longer appear, and an overall decrease in the intensity of (100) reflection is also observed. These changes are due to the decrease in

Table 1 Composition and textural parameters of samples

Samples	Composition				Textural parameters	
	C (wt%)	N (wt%)	Cr (wt%)	N/Cr ^a	S _{BET} (m ² /g)	d _p (nm)
Cr(Sal–Ala)	43.05 (43.09) ^b	5.00 (5.03) ^b	18.6 (18.67) ^b	0.99 (1.00) ^b	–	–
SiO ₂	–	–	–	–	327	9.73
MCM-41	–	–	–	–	1,050	2.76
SBA-15	–	–	–	–	712	7.61
Cr(Sal–Ala)–SiO ₂	5.08	0.91	1.7	1.99 (2.00) ^b	235	8.35
Cr(Sal–Ala)–MCM-41	5.38	0.97	1.8	2.00 (2.00) ^b	650	2.27
Cr(Sal–Ala)–SBA-15	5.10	0.92	1.7	2.01 (2.00) ^b	586	5.60
Cr(Sal–Ala)–SiO ₂ (CH ₃)	6.20	0.86	1.6	2.00 (2.00) ^b	210	7.52
Cr(Sal–Ala)–MCM-41(CH ₃)	7.26	0.87	1.6	2.02 (2.00) ^b	517	2.12
Cr(Sal–Ala)–MCM-41(CH ₃) ^c	6.81	0.82	1.5	2.03 (2.00) ^b	505	2.10
Cr(Sal–Ala)–SBA-15(CH ₃)	6.05	0.81	1.5	2.01 (2.00) ^b	485	5.36

^a Molar ratio

^b Value in parenthesis corresponds to the calculated results

^c The recovered catalyst after reusing six times

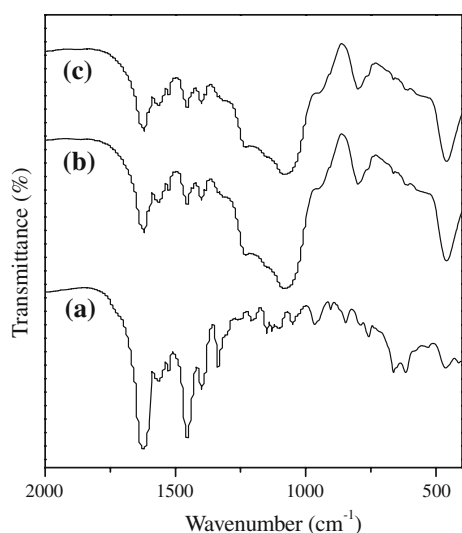


Fig. 3 FTIR spectra of (a) Cr(Sal-Ala), (b) Cr(Sal-Ala)-MCM-41, (c) Cr(Sal-Ala)-MCM-41(CH₃)

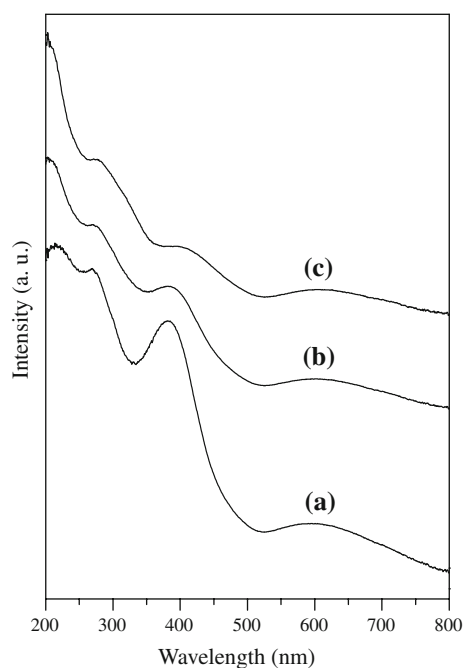
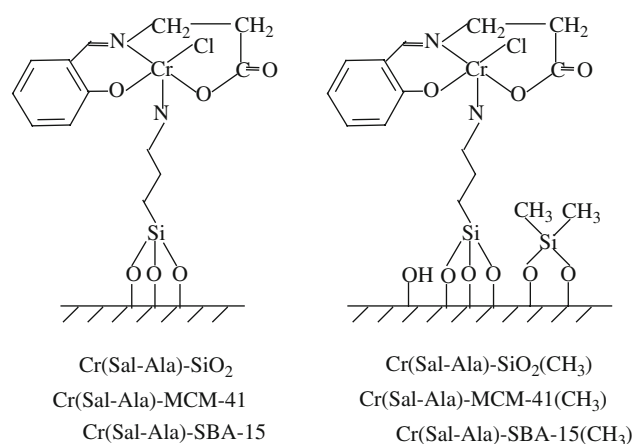


Fig. 4 UV-vis spectra of (a) Cr(Sal-Ala), (b) Cr(Sal-Ala)-MCM-41, (c) Cr(Sal-Ala)-MCM-41(CH₃)

local order as previously mentioned by Lim et al. [38]. Moreover, the (100) reflections of the immobilized complexes show clear shifts to higher 2θ values compared to those of the corresponding parent samples, which can be attributed to the contraction of the unit cells of the grafted samples originating from the immobilization of the bulky organometallic groups inside the channels of MCM-41 and SBA-15 [39, 40].

The N₂ adsorption-desorption isotherms of the three immobilized complexes all correspond to the type IV class



Scheme 1 Structural representation of the as-prepared immobilized chromium complexes

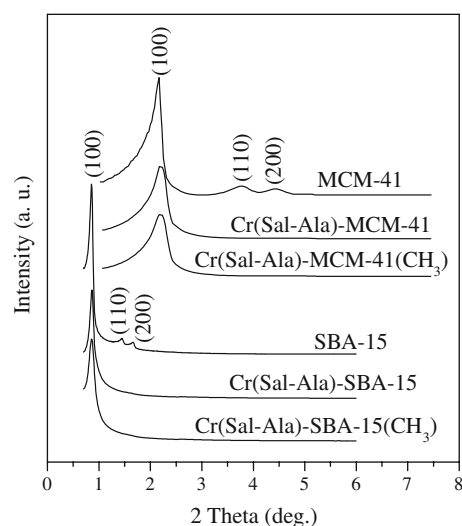


Fig. 5 XRD patterns of samples

of the IUPAC classification, suggesting that the mesosized structures of the supports remain intact after the immobilization of Cr(Sal-Ala) complex [41]. However, the immobilized materials all exhibit a decrease in surface area and pore size in comparison with their parent samples (see Table 1), which may be due to the attaching of organic moieties on the walls of the supports [42].

3.4 Surface Properties of Immobilized Complexes

The density of Cr(Sal-Ala) complexes per surface area in the two complexes immobilized on SiO₂ is two times higher than that on MCM-41 and on SBA-15 (see Table 2). This indicates a low dispersion of the active moieties in the complexes immobilized on SiO₂. Moreover, with the introduction of non-polar methyl groups, the amounts of polar residual silanol groups on the support surface of

Table 2 Surface group density of samples

Samples	Density of Cr(Sal–Ala) ($\times 10^{-6}$ mol/m ²)	Residual silanol groups ^a per gram sample ($\times 10^{-3}$ mol/g)	Water adsorbed ^b per gram sample (g/g)	Contact angle (°)
SiO ₂	–	2.2	0.10	–
Cr(Sal–Ala)–SiO ₂	1.39	1.0	0.09	–
Cr(Sal–Ala)–SiO ₂ (CH ₃)	1.47	0.6	0.07	92
MCM-41	–	5.0	0.12	–
Cr(Sal–Ala)–MCM-41	0.53	2.1	0.11	–
Cr(Sal–Ala)–MCM-41(CH ₃)	0.60	0.7	0.07	95
SBA-15	–	4.8	0.13	–
Cr(Sal–Ala)–SBA-15	0.56	2.0	0.11	–
Cr(Sal–Ala)–SBA-15(CH ₃)	0.59	0.6	0.08	97

^a Calculated from FTIR spectroscopy

^b The saturation adsorption capacities of water for samples were obtained from the adsorption isotherms of water

immobilized complexes decrease. So the surface polarity of immobilized complexes most likely decreases as well. Simultaneously, the amount of water adsorbed in the immobilized complexes decreases as the samples become richer in methyl groups, indicating that the hydrophobic character of the surface increases with the loading of methyl groups. However, a further study on the hydrophobicity of the three methyl-containing samples reveals that their contact angles for water are all less than 100° suggesting that they are only moderately hydrophobic. Thus, the introduction of methyl groups mainly leads to a modification in the surface polarity of the immobilized complexes.

3.5 Catalytic Performance

The so-obtained immobilized complexes and their homogeneous analogue were tested in the epoxidation of styrene with 30% H₂O₂. Six products, epoxide, benzaldehyde, hyacinth, hypnone, benzoic acid and benzyl benzoate were detected under the conditions used. The results in Table 3 reveal that only a small amount of epoxide (<5%) is produced in the absence of catalyst. With Cr(Sal–Ala) as catalyst, the styrene conversion and epoxide selectivity are slightly increased to 30.2 and 16.9%, respectively. However, when the reaction is performed over immobilized Schiff base complexes, the catalytic performance is found to be significantly improved, and the optimal epoxide yield reaches 61.8% over Cr(Sal–Ala)–MCM-41(CH₃). Such obviously enhanced catalytic performance, on the one hand, can be attributed to the dispersion effect of supports [23, 43–47]. Compared to the active sites in homogeneous systems, the dispersed catalytic sites in immobilized complexes exhibit more difficulty in forming the inactive μ -oxo dimers or other polymeric species. Thus, the immobilized complexes do not undergo rapid degradation

as their homogeneous analogue, and then exhibit significantly enhanced catalytic performance. On the other hand, the introduction of the support changes the local environment of active sites, and then influences the local concentration of the reactant and product around active sites, which in turn may contribute to the enhanced catalytic performance of immobilized complexes [26].

The differences in the catalytic performance of immobilized complexes with different supports were also investigated in detail, and the results are listed in Table 3. It is found that the two complexes immobilized on SiO₂ exhibit the worst catalytic performance. Simultaneously, the two complexes immobilized on SBA-15 exhibit relatively higher styrene conversion and much lower epoxide selectivity than the two complexes immobilized on MCM-41. Based on the yield of epoxide, the catalytic performance of the complexes immobilized on different supports decreases in the following order: on MCM-41 > on SBA-15 \gg on SiO₂.

A comparison of the immobilized complexes in terms of dispersion of their active complexes indicates that the poor catalytic performance of the complexes immobilized on SiO₂ can be attributed to the low dispersion of their active moieties as depicted in Table 2. The excessive active complexes per surface area in the complexes immobilized on SiO₂ also have probably formed the inactive polymers [23]. Considering that the complexes immobilized on MCM-41 and SBA-15 exhibit similar dispersion of active complexes, surface polarity and hydrophobicity, the significant differences in their catalytic performance can be reasonably related to the different channels and pore sizes of their supports. The different textural properties of the two supports might show different degrees of influence on the catalytic performance of the immobilized complexes through modifying the local amounts of reactant (styrene) and objective product (epoxide) around active sites [48].

Table 3 Catalytic performance of catalysts in the oxidation of styrene

Samples	Con. ^a (%)	Sel. ^b (%)						H ₂ O ₂ efficiency ^c (%)
		Epoxide	Benzaldehyde	Hyacinthin	Hypnone	Benzoic acid	Benzyl benzoate	
Blank	12.2	2.7	92.5	1.2	0	3.6	0	7.8
Cr(Sal–Ala)	30.2	16.9	75.7	2.4	1.5	2.8	0.7	20.1
Cr(Sal–Ala)–SiO ₂	43.6	35.1	50.3	5.6	2.1	4.7	2.2	32.8
Cr(Sal–Ala)–MCM-41	72.6	64.3	22.6	4.3	2.0	4.5	2.3	55.2
Cr(Sal–Ala)–SBA-15	73.0	61.5	23.3	4.0	2.5	5.5	3.2	58.5
Cr(Sal–Ala)–SiO ₂ (CH ₃)	51.5	44.3	42.8	4.5	2.1	5.0	1.3	44.5
Cr(Sal–Ala)–MCM-41(CH ₃)	80.2	77.0	16.5	2.2	0.6	3.5	0.2	74.6
Cr(Sal–Ala)–SBA-15(CH ₃)	85.8	67.2	19.1	3.7	2.0	5.6	2.4	75.0

Reaction conditions: Styrene 25 mmol, H₂O₂ 100 mmol, heterogenised catalyst 0.25 g or homogeneous catalyst 0.025 g, CH₃CN 10 mL, 0 °C, 4 h

^a Conversion = (moles of styrene reacted/moles of styrene in the feed) × 100

^b Selectivity = (moles of styrene converted to the products/moles of styrene reacted) × 100

^c Efficiency of H₂O₂ for styrene oxidation = (moles of H₂O₂ converted to the products/moles of H₂O₂ consumed) × 100

Table 4 Adsorption of styrene and epoxide with different samples

Samples	Adsorption of styrene (×10 ⁻⁶ mol/g)	Adsorption of epoxide (×10 ⁻⁶ mol/g)
Cr(Sal–Ala)–SiO ₂	1.34	1.55
Cr(Sal–Ala)–MCM-41	1.28	1.51
Cr(Sal–Ala)–SBA-15	1.36	1.60
Cr(Sal–Ala)–SiO ₂ (CH ₃)	1.22	1.26
Cr(Sal–Ala)–MCM-41(CH ₃)	1.20	1.25
Cr(Sal–Ala)–SBA-15(CH ₃)	1.25	1.31

Here, a series of adsorption tests were designed to investigate the local amounts of styrene and epoxide molecules around active sites by UV–Vis spectroscopy. The results reveal that the two complexes immobilized on SBA-15 both display higher adsorption capacities for styrene and epoxide than their corresponding complexes immobilized on MCM-41 (see Table 4). This may be related to the crossed channels and big pore sizes of SBA-15, which facilitate the adsorption of styrene and epoxide. The results of the adsorption tests indicate that more styrene molecules can access the active sites in the complexes immobilized on SBA-15, so the immobilized complexes exhibit much higher styrene conversion. However, the much higher adsorption capacities for epoxide of the complexes immobilized on SBA-15 simultaneously increase the probability of this object product being overoxidized, thus a relatively lower selectivity to epoxide is obtained.

Furthermore, the results in Table 3 also display that the introduction of hydrophobic methyl groups lead to an improvement in the H₂O₂ efficiency and the catalytic performance of immobilized complexes independent of the supports used. Such an improvement might be attributed to

the modification in the surface properties of immobilized complexes originating from the methyl groups which further influence the access of styrene and epoxide molecules to the active sites [49]. Thus, we investigated in detail the differences in the adsorption capacities of immobilized complexes with or without methyl groups for styrene and epoxide. Upon the introduction of methyl groups, the adsorption capacities of immobilized complexes for styrene only show a moderate decrease, while a sharp decrease in their adsorption capacities for epoxide is observed (see Table 4). Such differences in the adsorption capacities may be due to the different polarity of styrene and epoxide. As mentioned above, with the introduction of methyl groups, the surface polarity of immobilized complexes significantly decreases, so their adsorption capacities for epoxide with higher polarity tend to sharply decrease as well. This also indicates that the amount of epoxide accessible to active sites of methyl-containing immobilized complexes significantly decreases. Thus, the probability of the freshly produced epoxide being overoxidized decreases, which could afford the significantly improved epoxide selectivity in the presence of methyl-containing catalysts. Simultaneously, the moderate decrease in the adsorption capacities of methyl-containing immobilized complexes for styrene indicates that the styrene molecules had more difficulty to access the active sites of methyl-containing catalysts. In this respect, the methyl-containing catalysts should exhibit relatively lower styrene conversion, which is contrary to the factual results. Thus, the enhanced styrene conversion is mainly attributed to the improved H₂O₂ efficiency, and consequently to the decreased amount of residual silanol groups in methyl-containing immobilized complexes. We have discussed the correlation between the H₂O₂ efficiency, the conversion of

reactant and the amounts of residual silanol groups in our previous report [29].

In order to obtain the best catalytic results, the effect of condition parameters on the catalytic performance of Cr(Sal-Ala)-MCM-41(CH₃), which is the most active catalyst in the epoxidation of styrene among all immobilized materials, was investigated. It is found that the dosage of oxidant, the reaction time and temperature all significantly influence the catalytic performance of this immobilized complex (see Fig. 6). When the reaction ran for 4 h at 0 °C with a H₂O₂/styrene molar ratio of 4, the best styrene conversion is of 80.2% with 77.0% selectivity to epoxide, and the main byproduct is benzaldehyde with 16.5% selectivity.

The mechanistic probe for the epoxidation of olefins with peroxide by oxometal complexes is attracting continuous interest, and the prevailing accepted views are the enzyme mimetic mechanism (the heterolytic bond cleavage of peroxide) and the free-radical mechanism (the homolytic bond cleavage of peroxide). Generally, the heterolytic bond cleavage of peroxide tends to form epoxide [50, 51]. In the

present investigation, epoxide is found to be the major product, indicating that the hydroperoxide O–O bond is mainly cleaved heterolytically. Accordingly, the coordinatively unsaturated chromium (III) mainly seems to activate H₂O₂ via heterolytic cleavage of the peroxide bond resulting in high-valent oxochromium (V) intermediate, and then reacts with styrene to yield epoxide.

In addition, a further study on the stability of Cr(Sal-Ala)-MCM-41(CH₃) was also carried out. After the first catalytic run, this immobilized catalyst was separated from the reaction solution, washed several times with solvent to remove any physisorbed molecules, dried and then reused in another five catalytic runs. The results in Fig. 7 reveal that the catalyst is still active up to six times of reusage, however, with the further increase in the reusage, the catalytic performance decreases significantly. The elemental composition and textural properties of the recovered catalyst after six times were also investigated, and the results are listed in Table 1. The recovered catalyst reveals almost the same elemental composition as the fresh catalyst, indicating that the anchoring between chromium

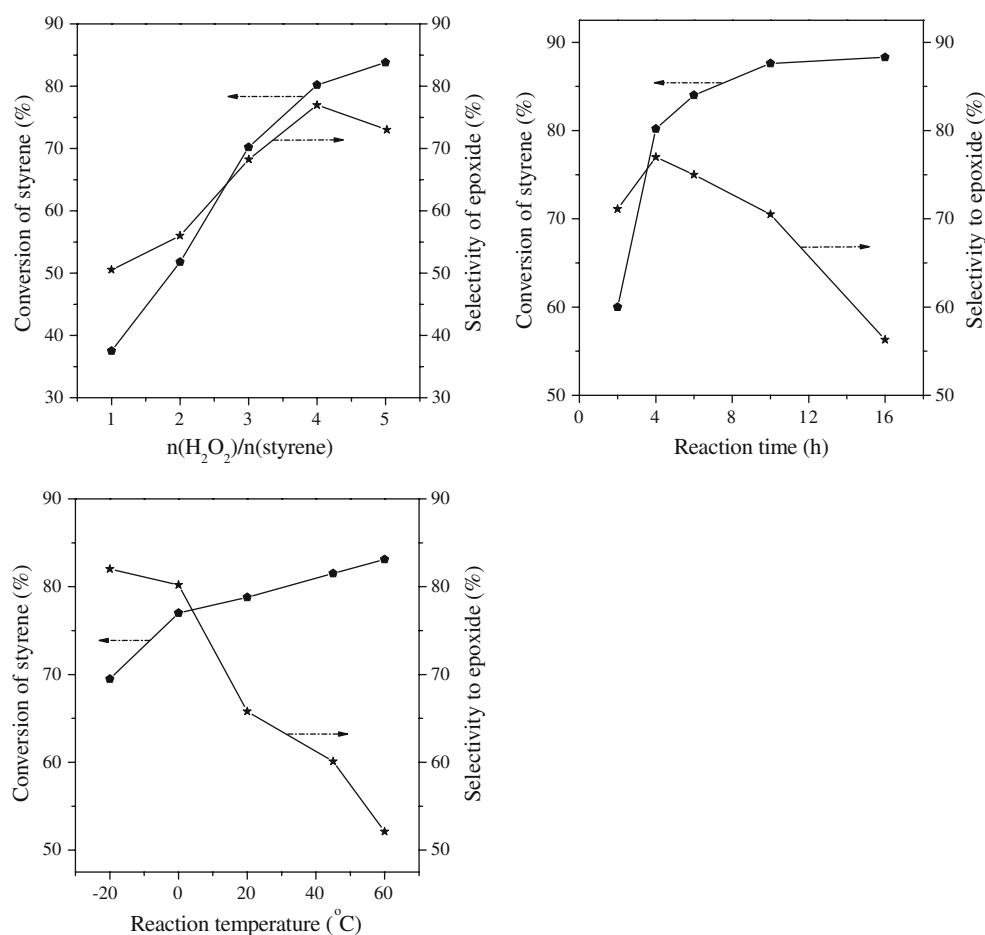


Fig. 6 Effect of condition parameters on the catalytic performance of Cr(Sal-Ala)-MCM-41(CH₃). Reaction conditions: Styrene 25 mmol, catalyst 0.25 g, CH₃CN 10 mL

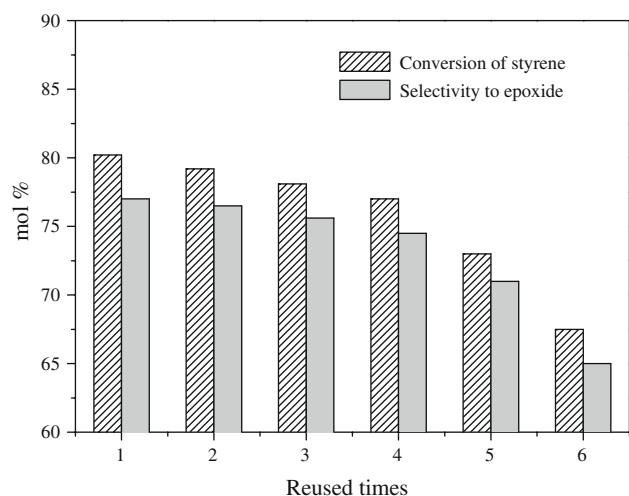


Fig. 7 Reusability of Cr(Sal-Ala)-MCM-41(CH₃). Reaction conditions: Styrene 25 mmol, H₂O₂ 100 mmol, catalyst 0.25 g, CH₃CN 10 mL, 0 °C, 4 h

complexes and support is strong enough to afford six catalytic runs, and the chromium leaching is negligible. Therefore, the decreasing catalytic performance over the recovered catalyst with increasing catalytic runs may be reasonably attributed to the increasing residual adsorbed molecules which prevent the reactants from accessing the active sites. This is confirmed by the decreased surface areas and pore sizes of the recovered catalyst in comparison with the fresh catalyst due to the attaching of residual adsorbed molecules to the walls of support. The obtained immobilized complexes here also encounter the problem of recycling in more catalytic runs for immobilized catalysts prepared by coordinatively bonding active sites on the support, and similar phenomena have been reported previously [25]. Thus, further increasing the stability of such promising oxidative catalyst will be the focus of our following work, which we think is of significance for highly effective heterogeneous catalyst design.

4 Conclusions

A series of alanine-salicylaldehyde Schiff base chromium (III) complexes immobilized on three typical mesoporous supports (SiO₂, MCM-41 and SBA-15) were prepared, and they exhibited promising catalytic performance towards the epoxidation of styrene with 30% H₂O₂. The textural properties of the supports such as the surface area, channels and pore sizes were found to play important roles in the catalytic performance of the resulting immobilized complexes. Simultaneously, the further introduction of methyl groups significantly improved the catalytic performance of immobilized complexes by modifying their surface

properties. The best styrene conversion reached 80.2% with 77.0% selectivity to epoxide over Cr(Sal-Ala)-MCM-41(CH₃), and the main byproduct was benzaldehyde (Selectivity 16.5%). In addition, this immobilized material could be reused for several runs.

Acknowledgements The authors acknowledge the financial supports from National Science Technology Foundation of China (No. 2006BAC2A08) and NJIT Scientific Research Foundation for Introduce Talents (KXJ 08033 and KXJ 08034).

References

- Mandelli D, van Vliet MCA, Arnold U, Sheldon RA, Schuchardt U (2001) *J Mol Catal A* 168:165
- Ishii Y, Yamawaki K, Ura T, Yamada H, Yoshida T, Ogawa M (1988) *J Org Chem* 53:3587
- De Vos DE, Sels BF, Reynaers M, Subba Rao YV, Jacobs PA (1998) *Tetrahedron Lett* 39:3221
- Copéret C, Adolfsson H, Sharpless KB (1997) *Chem Commun* 1565
- Rudler H, Gregorio JR, Denise B, Brégeault J-M, Deloffre A (1998) *J Mol Catal A* 133:255
- van Vliet MCA, Arends IWCE, Sheldon RA (1999) *Chem Commun* 821
- Herrmann WA, Fischer RW, Marz DW (1991) *Angew Chem Int Ed* 30:1638
- Herrmann WA, Eder SJ, Kiprof P (1991) *J Organomet Chem* 412:407
- Tsuji Y, Ohta T, Ido T, Minbu H, Watanabe Y (1984) *J Organomet Chem* 270:333
- Barak G, Dakka J, Sasson Y (1988) *J Org Chem* 53:3553
- Marko IE, Gautier A, Chelle-Regnaut I, Giles PR, Tsukazaki M, Urch CJ, Brown SM (1998) *J Org Chem* 63:7576
- Fernández I, Pedro JR, Roselló AL, Ruiz R, Castro I, Ottenwelder X, Journaux Y (2001) *Eur J Org Chem* 7:1235
- Wang RM, Hao CJ, He YF, Wang YP, Xia CG (2002) *Polym Adv Technol* 13:6
- Zhao J, Han J, Zhang YC (2005) *J Mol Catal A* 231:129
- Abdi SHR, Kureshy RI, Khan NH, Jasra RV (2004) *Catal Surv Jpn* 8:187
- Halligudi SB, Devassy BM, Kala Raj NK, Degaonkar MP, Gopinathan S (2000) *React Kinet Catal Lett* 71:289
- Yang DH, Gao L, Zhao WJ (2008) *Catal Lett* 126:84
- Bahramian B, Mirkhani V, Moghadam M, Tangestaninejad S (2006) *Catal Commun* 7:289
- Abrantes M, Sakthivel A, Romão CC, Kühn FE (2006) *J Organomet Chem* 691:3137
- Baleizão C, Gigante B, Garcia H, Corma A (2003) *J Catal* 215:199
- Luts T, Suprun W, Hofmann D, Klepel O, Papp H (2006) *J Mol Catal A* 261:16
- Zhou XG, Yu XQ, Huang JS, Li SG, Li LS, Che CM (1999) *Chem Commun* 1789
- Lau S-H, Caps V, Yeung K-W, Wong K-Y, Tsang SC (1999) *Microporous Mesoporous Mater* 32:279
- Corma A, Garcia H, Moussaif A, Sabater MJ, Zhiber R, Redouane A (2002) *Chem Commun* 1058
- Baleizão C, Gigante B, Sabater MJ, Garcia H, Corma A (2002) *Appl Catal A* 228:279

26. Wang XL, Wu GD, Li JP, Zhao N, Wei W, Sun YH (2007) *J Mol Catal A* 276:86
27. Kresge CT, Leonowicz ME, Roth WJ, Vartuli JC, Beck JS (1992) *Nature* 359:710
28. Zhao DY, Feng JL, Huo QS, Melosh N, Fredrickson GH, Chmelka BF, Stucky GD (1998) *Science* 279:548
29. Wang XL, Wu GD, Li JP, Zhao N, Wei W, Sun YH (2007) *Catal Lett* 119:89
30. Heinert D, Martell AE (1962) *J Am Chem Soc* 84:3257
31. Shanthi R, Nagaraja KS, Udupa MR (1987) *Inorg Chem Acta* 133:211
32. Bikerman JJ (1958) *Surface chemistry: theory and applications*, 2nd edn. Academic Press, New York, p 343
33. Carvalho WA, Wallau M, Schuchardt U (1999) *J Mol Catal A* 144:91
34. Sindorf DW, Maciel GE (1981) *J Am Chem Soc* 103:4263
35. Díaz I, Márquez-Alvarez C, Mohino F, Pérez-Pariente J, Sastre E (2000) *J Catal* 193:283
36. Percy GC (1975) *J Inorg Nucl Chem* 37:2071
37. Ren T, Yan L, Zhang HP, Suo JS (2003) *J Mol Catal (China)* 19:310
38. Lim MH, Stein A (1999) *Chem Mater* 11:3285
39. Sakthivel A, Zhao J, Hanzlik M, Chiang AST, Herrmann WA, Kühn FE (2005) *Adv Synth Catal* 347:473
40. Jia MJ, Seifert A, Berger M, Giegengack H, Schulze S, Thiel WR (2004) *Chem Mater* 16:877
41. Sing KSW, Everett DH, Haul RAW, Moscow L, Pierotti RA, Rouquerol T, Siemieniowska T (1985) *Pure Appl Chem* 57:603
42. Brunel D, Bellocq N, Sutra P, Cauvel A, Laspéras M, Moreau P, Renzo FD, Galarneau A, Fajula F (1998) *Coord Chem Rev* 180:1085
43. Karandikar P, Dhanya KC, Deshpande S, Chandwadkar AJ, Sivasanker S, Agashe M (2004) *Catal Commun* 5:69
44. Belal R, Meunier B, Aurangzeb N (1988) *J Mol Catal A* 44:187
45. Aurangzeb N (1994) *J Chem Soc Chem Commun* 1153
46. Silva AR, Figueiredo JL, Freire C, de Castro B (2004) *Microporous Mesoporous Mater* 68:83
47. Joseph T, Hartmann M, Ernst S, Halligudi SB (2004) *J Mol Catal A* 207:131
48. Maldotti A, Molinari A, Varani G, Lenarda M, Storara L, Bigi F, Maggi R, Mazzacani A, Sartori G (2002) *J Catal* 209:210
49. Corma A, Domine M, Gaona JA, Jordá JL, Navarro MT, Rey F, Pérez-Pariente J, Tsuji J, McCulloch B, Nemeth LT (1998) *Chem Commun* 2211
50. Nam W, Choi HJ, Han HJ, Cho SH, Lee HJ, Han SY (1999) *Chem Commun* 387
51. Liu CJ, Yu WY, Li SG, Che CM (1998) *J Org Chem* 63:7364